

Direct Observation of 3D Mesoporous Structure by Scanning Electron Microscopy (SEM): SBA-15 Silica and CMK-5 Carbon**

Shunai Che, Kristina Lund, Takashi Tatsumi, Sumio Iijima, Sang Hoon Joo, Ryong Ryoo, and Osamu Terasaki*

Mesoporous silica has attracted much attention in recent years, because of its potential for advanced applications in catalysis, separation technologies, electronic engineering, and manufacturing of optical devices.^[1,2] The highly nanoporous structures with good thermochemical stability are suitable for the synthesis of new materials such as nanoparticles, wires and networks of platinum and carbon within the pore system.^[3,4] In the case of the carbon synthesis, the fabrication technique has been fully developed so that ordered mesoporous carbons exhibiting Bragg X-ray diffraction (XRD) lines similar to those of the MCM-41-type mesoporous silica can be obtained after the complete removal of the silica template.

Recently, an electron crystallographic analysis method based on transmission electron microscopy (TEM) has been developed to solve 3D structures of mesoporous silica crystals.^[5] The structural solution provided direct information

on detailed structures inside the mesoporous crystals such as pore diameter, shape and connectivity. But, the detailed structures at the crystal surfaces, such as the manner of channel openings at external surface and the accessibility to internal pores, were not clarified. Scanning electron microscopy (SEM) has advantages over TEM for the determination of the surface structures. SEM is a relatively simple experiment and requires minimum sample preparation, and solid information on surface structures can be obtained from “nonprojected” images in three dimensions because of the long focal depth of the objective lens.^[6] However, because of “charging problems” common for insulators and low resolution, ordinary SEM has been unsuitable for accurate determination of the detailed surface structures of the mesoporous materials.

Herein, we report that we can visualize directly the detailed surface structures of the SBA-15 mesoporous silica and its CMK-5 carbon replica, by using high resolution SEM and scanning transition electron microscopy (STEM) without metal coating. The high-resolution 3D SEM images clearly show the presence of interconnections between the hexagonally packed mesoporous channels, as suggested in previous works based on TEM imaging of the Pt replica.^[4,7] Interestingly, the images show that the surfaces perpendicular to the direction of the channels (*c* direction) are intricately composed of tubes with closed ends, open ends, and channels that are curled back to the inside of the particles. Furthermore, we can distinguish two types of pores in the CMK-5 carbon, that is, the tubelike pores formed by carbon tubes and pores formed by removal of the silica wall.

The SBA-15 silica and CMK-5 carbon samples observed in the SEM investigation were obtained by following procedures described elsewhere.^[3a] Typical synthesis conditions and properties obtained from N₂ adsorption–desorption measurement are given in Table 1.

Figure 1 shows SEM images and STEM image of the calcined SBA-15 silica sample. The silica particles in the SEM image exhibit hexagonal cylinderlike morphologies with curvatures along the *c* direction, which is consistent with the 2D hexagonal mesostructures. The high-resolution SEM images reveal that the external surfaces parallel to the *c* direction are composed of a uniform array of bisectonal parts of channels. The channel walls exhibit “wiggling” along the *c* direction to form random interconnections between adjacent channels. However, compared to the surfaces parallel to the *c* direction, the external surfaces perpendicular to the *c* direction is composed of intricately curved channels. Many of the channels are curled to join back with others at the surfaces.

The STEM analysis was performed with microtomed cross sections of the particles. The STEM image confirms that the channels are hexagonally arranged within the hexagonal cylinder, and that the channels at surfaces along the *c* direction have a concaved open cross-sectional shape (Figure 1e). The image analysis gave the SBA-15 pore diameters in the range of 7.5 ± 0.3 nm and the thickness of the pore wall to be 2.5 ± 0.3 nm. A schematic model of the structure is given in Figure 2, the interconnections of channels are not shown for simplicity. It can be considered that the surface of the

[*] Dr. O. Terasaki
Department of Physics
Graduate School of Science
Tohoku University
Sendai, 980-8578 (Japan)
Fax: (+81) 22-217-6475
E-mail: terasaki@struc.su.se
E-mail: terasaki@msp.phys.tohoku.ac.jp

S. Che, S. Iijima
ICORP-JST
c/o NEC
34 Miyukigaoka, Tsukuba, Ibaraki, 305-8501 (Japan)

Dr. O. Terasaki, K. Lund
Arrhenius Laboratory
Stockholm University
10691 Stockholm (Sweden)

S. Che, T. Tatsumi
Division of Materials Science & Chemical Engineering
Faculty of Engineering
Yokohama National University
79-5 Tokiwadai, Yokohama 240-8501 (Japan)

S. H. Joo, R. Ryoo
National Creative Research Initiative Center for Functional Nanomaterials and
Department of Chemistry (School of Molecular Science-BK21)
Korea Advanced Institute of Science and Technology
Daejeon, 305-701 (Korea)

[**] The authors are grateful to Messrs Makoto Watanabe (Hitachi Science System) and Yasushi Nakaizumi (Hitachi High-Technologies Corporation) for taking scanning electron micrographs. S.C. thanks Dr. M. Yudasaka (ICORP-JST) for giving advise and comments.

Table 1: Properties of tubelike mesoporous carbon materials with different tube diameters.

| Sample | Synthesis conditions | | Unit cell a [nm] | Surface area S_{BET} [m ² g ⁻¹] ^[a] | Tube diameter d_{BJH} [nm] ^[b] |
|------------------|----------------------|---------------------|--------------------|--|--|
| | FA/SiO ₂ | Polymerization time | | | |
| SBA-15 | – | – | 9.8 | 597 | 8.2 ^[c] |
| a | 1.5 | 2 h | 9.4 | 1750 | 5.0 |
| b | 1.5 | 3 h | 9.8 | 1640 | 4.6 |
| c | 2.0 | 4 h | 9.4 | 1578 | 4.2 |
| d | 2.5 | 6 h | 9.6 | 1368 | 3.6 |
| e | 2.75 | – ^[e] | 9.4 | 1354 | 3.6 |
| f ^[d] | 3.25 | – ^[e] | 9.4 | 1118 | 3.0 |

[a] Calculated by the BET method. [b] Calculated from the adsorption branch of the N₂ isotherm of the CMK-5 without removing silica wall by using the BJH method. [c] Mesopore diameter of SBA-15. [d] Synthesized with two-step FA polymerization. [e] Synthesized without evacuation.

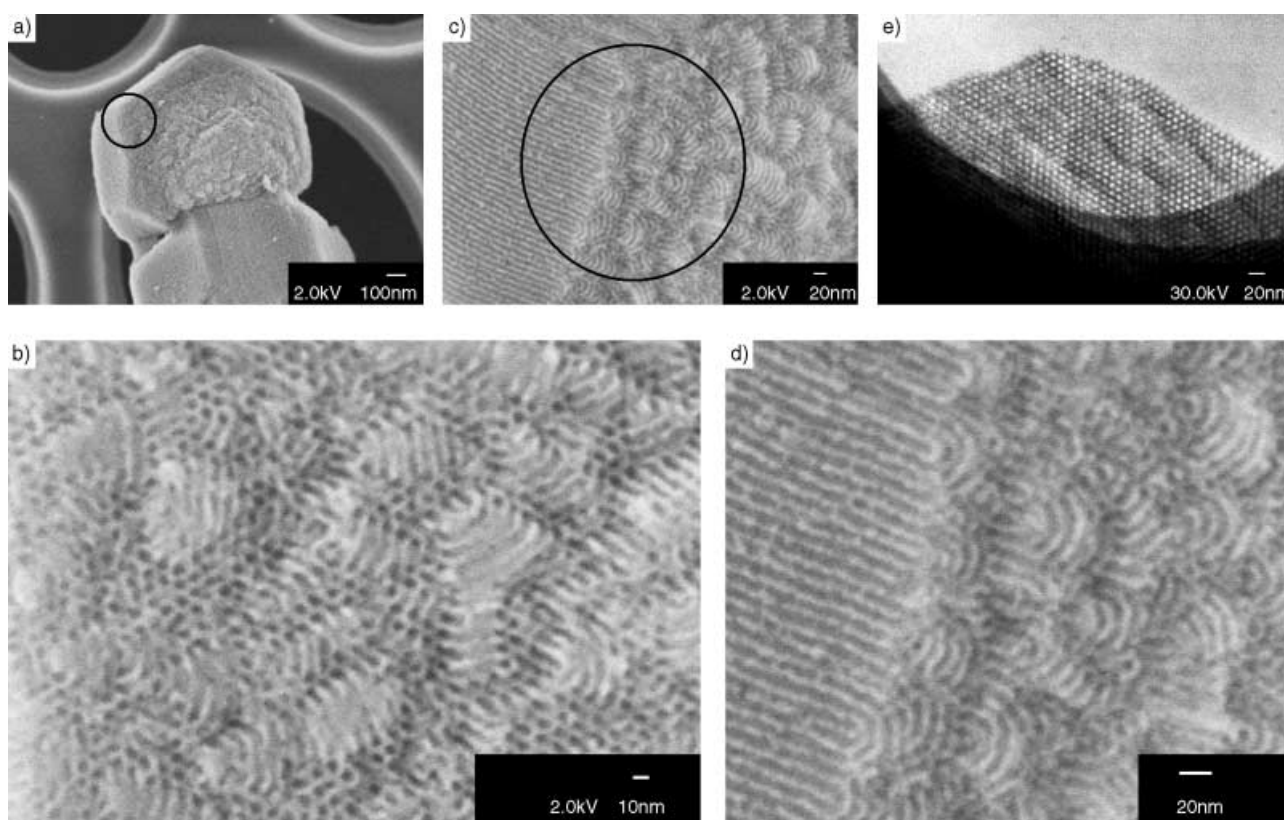


Figure 1. SEM (a, b, c and d) and STEM (e) images of SBA-15 mesoporous silica. Circled areas in a) and c) are enlarged in b) and d) respectively.

hexagonal cylinders along the c direction is always formed by the cut along the center of the pores. If the surfaces were formed by cuts along the pore walls (dotted line in Figure 2), we would not be able to observe the open concave channels. Initially, SBA-15 was considered to be an extra-large pore MCM-41 analogue with 2D hexagonal $p6mm$ structure. Later, the replication studies using platinum and carbon have revealed that the main channels of SBA-15 can be interconnected into the form of a 3D porous network,^[3,4,7] particularly when the synthesis mixture is heated after the mesophase formation.^[8]

Figure 3A and 3B show the XRD patterns of SBA-15 silica and CMK-5 carbons, which were synthesized with various ratios of furfuryl alcohol (FA)/silica and different times for FA polymerization. We found out that the tube inner diameter of the carbon product depended not only on the FA/silica ratio but also on the polymerization time before evacuation. At present, by using SBA-15 with pore diameter of 8.2 nm we were able to control the inner diameters of the CMK-5 carbon in the range of 3.0–5.0 nm (see Table 1). This result indicates that the thinnest possible tubes were 1.6 nm in wall thickness. Interestingly, it was difficult to prepare carbon

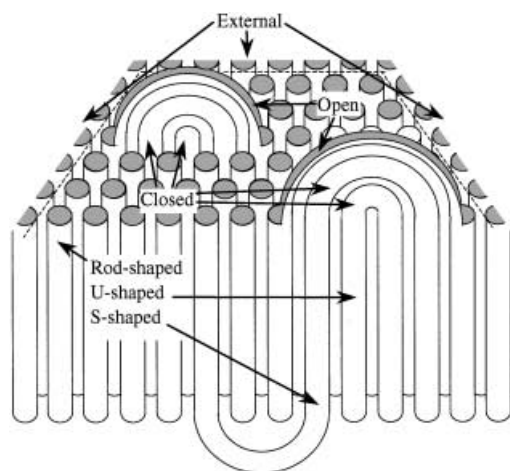


Figure 2. Schematic representation of the mesostructure of the SBA-15. Interconnections between adjacent channels are omitted for clarity.

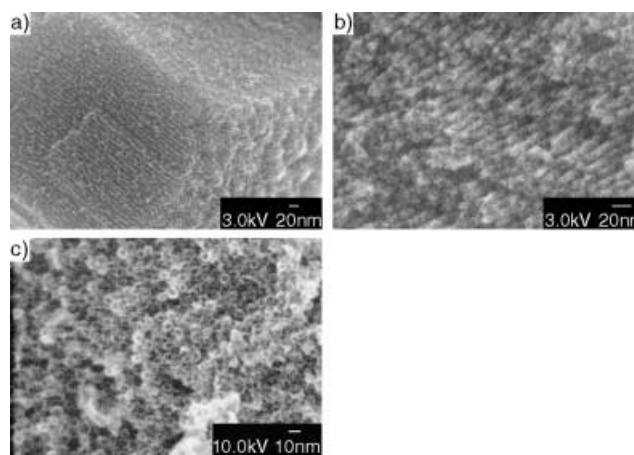


Figure 4. SEM images taken along different directions, at different magnifications and accelerating voltages from CMK-5 with tube inner diameter of 4.2 nm.

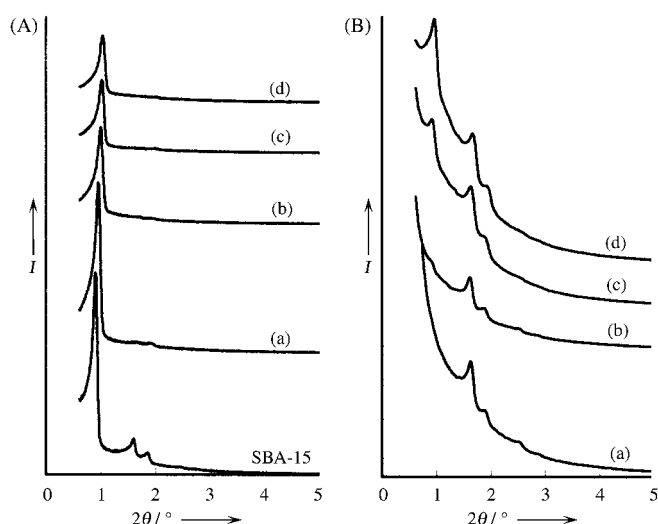


Figure 3. XRD patterns of SBA-15 and CMK-5 carbons obtained before (A) and after (B) removing silica wall. The FA/SiO₂ ratio and other synthesis conditions are a) 1.25:1, without evacuation; b) 1.5:1, with 3 h polymerization; c) 2.5:1, with 6 h polymerization; d) 3.25:1, with two steps FA polymerization; *I* = relative intensity.

tubes less than 3.6 nm in diameter by a single-step FA polymerization even by using a large amount of FA and without evacuation. When FA polymerization was performed in two steps, the tube diameter of the resultant CMK-5 was decreased to 3.0 nm. Oxalic acid was used as an acid catalyst for FA polymerization in the second step. We clearly observed that powder XRD intensity of the silica/carbon composite (i.e., samples just before removal of the silica framework) varied significantly depending on the thickness of the carbon tubes formed within the silica channels. More systematic studies on this point are continuing and the results will be reported separately.

Figure 4 shows the high-resolution SEM images of the CMK-5 sample with the inner diameter of 4.2 nm. The SEM images of the carbon exhibit very similar morphologies to those for the SBA-15 silica template. Interestingly, most of the carbon nanotubes are open at the surfaces of the porous crystals. This SEM investigation confirms that the carbon replication with FA can be perfectly achieved throughout the entire volume of the silica particle.

In conclusion, we have demonstrated for the first time that the resolution of the present SEM (taken directly from silica without gold plating) and STEM is sufficiently high for accurate determination of the surface structures of the mesostructured SBA-15 silica and CMK-5 carbon materials. We believe that these EM techniques can also be used for other mesoporous materials. The accurate information thus obtained will be highly useful for gaining new insights into the molecular factors governing the formation and growth of the inorganic–organic mesophases, and also for the development of various applications.

Experimental Section

SBA-15: SBA-15 mesoporous silica was synthesized by using the triblock copolymer Pluronic P123 (EO₂₀PO₇₀EO₂₀, *M*_{av} = 5800, BASF) as a surfactant and tetraethoxysilicon (TEOS) as a silica source. In a typical synthesis experiment, TEOS (20.8 g) was added to a mixture of P123 (10 g), TMB (0–20 g), HCl (62.57 g, 35 wt %), and deionized water (319 g) under static condition at 35°C. After the mixture was stirred for 24 h, the mesostructured product thus formed was cured at 100°C for an additional 24 h. The products were filtered, dried without washing, and calcined at 823 K.

CMK-5: CMK-5 was synthesized by using SBA-15 as the template and furfuryl alcohol (FA, C₅H₆O₂) as the carbon precursor. The SBA-15 silica was converted to an aluminosilicate form with a Si/Al ratio of 20:1, following the postsynthesis incorporative procedure. The pore volume of SBA-15 was filled with different amount of FA by the incipient-wetness technique. The aluminosilicate SBA-15 containing the FA was heated for different polymerization times (see Table 1) at 80°C and then at 150°C for 8 h, which resulted in the aluminosilicate acid-catalyzed polymerization of the FA in the form

of a layer coated on the pore walls. The remaining FA in the core of the template pores was removed by heating the sample at 80 °C with evacuation (Table 1 samples a, b, c, d) or without evacuation (Table 1 samples e, f). To obtain the smaller tube diameter, a two-step method was employed for the filling of FA. Oxalic acid was used as an acid catalyst in the second step, because the aluminosilicate wall was covered with FA polymer in the first step and therefore could not catalyze the polymerization further. The polymerized FA was converted to carbon inside the SBA-15 template by pyrolysis at 900 °C for 6 h under an Ar flow. The porous carbon was obtained after subsequent dissolution of the silica framework in 5% HF acid at room temperature.

XRD measurement: XRD patterns were recorded by using an MX Labo powder diffractometer equipped with $\text{CuK}\alpha$ radiation (40 kV, 20 mA) at the rate of $1.0^\circ \text{min}^{-1}$ over the range of $1.5\text{--}10.0^\circ$ (2θ). The samples were prepared as thin layers on glass slides.

SEM and STEM measurement: The microscopic features of all samples (Aluminated SBA-15, CMK-5 with different tube diameter) were observed with SEM (Hitachi, S-5200). To observe genuine pore structures on the external surface, the samples were observed without any metal coating for SEM. By using a low accelerating voltage, we can obtain selective information from the surface region. In addition, the “charging problems common for insulators” are not serious. The resolution is limited by an effective electron probe size on the specimen, and is determined from spreads owing to a) diffraction of an aperture (Airy pattern), b) spherical aberration, and c) chromatic aberration in addition to electron source size, therefore to obtain high-resolution images at low accelerating voltage an electron source with high brightness and coherence, and small spherical and chromatic aberrations of the objective lens are important.^[6] An accelerating voltage, 2 kV (resolution: ca. 1.2 nm) was chosen for SBA-15, because this was the highest possible without charging problem, and 10 kV (resolution: ca. 0.6 nm) for CMK-5 to optimize a relation between surface information and image resolution. To observe internal structures of the samples, STEM images were taken from thinly sectioned samples, mesoporous silica or carbon particles, obtained with an ultramicrotome.

N_2 adsorption-desorption measurement: The surface area and the pore size were measured at -196°C on a Belsorp 28SA sorption-meter. Samples were pretreated for 2 h at 200°C and 1.33×10^{-4} Pa. The BET specific surface area, S_{BET} , was calculated by using adsorption branches in the relative pressure range from 0.04 to 0.1. The primary mesopore volume V_p was obtained by using the high-resolution t-plot method. The pore size distribution was calculated from adsorption branches of isotherms using the BJH method.

Received: December 9, 2002 [Z50726]

Keywords: carbon nanotubes · electron microscopy · mesoporous materials · self-assembly · zeolite analogues

- [1] a) T. Yanagisawa, T. Shimizu, K. Kuroda, D. Kato, *Bull. Chem. Soc. Jpn.* **1990**, *63*, 988; b) C. T. Kresge, M. E. Leonowicz, W. J. Roth, J. C. Vartuli, J. S. Beck, *Nature* **1992**, *359*, 710; c) J. S. Beck, J. C. Vartuli, W. J. Roth, M. E. Leonowicz, C. T. Kresge, K. D. Schmitt, C. T.-W. Chu, D. H. Olson, E. W. Sheppard, S. B. McCullen, J. B. Higgins, J. L. Schlenker, *J. Am. Chem. Soc.* **1992**, *114*, 10834.
- [2] A. Monnier, F. Schüth, Q. Huo, D. Kumar, D. I. Margolese, R. S. Maxwell, G. D. Stucky, M. Krishnamurty, P. Petroff, A. Firouzi, M. Janicke, B. F. Chmelka, *Science* **1993**, *261*, 1299.
- [3] a) S. H. Joo, S. J. Choi, I. Oh, J. Kwak, Z. Liu, O. Terasaki, R. Ryoo, *Nature* **2001**, *412*, 169; b) R. Ryoo, S. H. Joo, S. Jun, *J. Phys. Chem. B* **1999**, *103*, 7743; c) S. Jun, S. H. Joo, R. Ryoo, M. Kruk, M. Jaroniec, Z. Liu, T. Ohsuna, O. Terasaki, *J. Am. Chem. Soc.* **2000**, *122*, 10712.

- [4] a) Z. Liu, O. Terasaki, T. Ohsuna, K. Hiraga, H. J. Shin, R. Ryoo, *ChemPhysChem* **2001**, *2*, 229; b) O. Terasaki, Z. Liu, T. Ohsuna, H. J. Shin, R. Ryoo, *Microsc. Microanal.* **2002**, *8*, 35; c) H. J. Shin, C. H. Ko, R. Ryoo, *J. Mater. Chem.* **2001**, *11*, 260.
- [5] a) A. Carlsson, M. Kaneda, Y. Sakamoto, O. Terasaki, R. Ryoo, S. H. Joo, *J. Electron Microsc.* **1999**, *48*, 795; b) Y. Sakamoto, M. Kaneda, O. Terasaki, D. Y. Zhao, J. M. Kim, G. Stucky, H. J. Shin, R. Ryoo, *Nature* **2000**, *408*, 449; c) M. Kaneda, T. Tsubakiyama, A. Carlsson, Y. Sakamoto, T. Ohsuna, O. Terasaki, S. H. Joo, R. Ryoo, *J. Phys. Chem. B* **2002**, *106*, 1256.
- [6] “Structure and Structure Determination”: O. Terasaki in *Electron Microscopy Studies in Molecular Sieve Science in Molecular Sieves-Science and Technology, Vol. 2* (Eds.: H. G. Karge, J. Weitkamp), Springer, Heidelberg, **1999**, p. 71–112.
- [7] R. Ryoo, C. H. Ko, M. Kruk, V. Antochshuk, M. Jaroniec, *J. Phys. Chem. B* **2000**, *104*, 11465.
- [8] A. Galarneau, H. Cambon, F. Di. Renzo, R. Ryoo, M. Choi, F. Fajula, *New J. Chem.* **2003**, *27*, 73.